



1
2 **Continuous *in situ* monitoring of the vertical and horizontal passage of a labeled-water pulse**
3 **through a boreal Scots pine forest**

4 John D. Marshall^{1,2,3}, Maren Dubbert⁴, Teresa E. Gimeno⁵, Ruth-Kristina Magh^{6,2}, Kathrin
5 Kühnhammer⁷, David Dubbert⁴, Paul Koeniger⁸, Matthias Cuntz⁹, Matthias Beyer¹⁰

6 ¹Department of Geosciences, University of Gothenburg, Gothenburg, Sweden

7
8 ²Forest Ecology and Management, Swedish University of Agricultural Sciences (SLU), SE-901 83
9 Umeå, Sweden

10 ³Department of Matters and Energy Fluxes, Global Change Research Institute, 60300 Brno, Czechia

11 ⁴Isotope Biogeochemistry and Gas Fluxes, Leibniz Institute for Agricultural and Landscape Research
12 (ZALF), 15374 Müncheberg, Germany

13
14 ⁵CREAF, 08193 Bellaterra (Cerdanyola del Vallès), Catalonia, Spain,

15 ⁶Terrestrial Ecohydrology, Friedrich Schiller University, 07749 Jena, Germany

16 ⁷Ecosystem Physiology, Albert-Ludwigs-Universität Freiburg, Germany

17
18 ⁸Federal Institute for Geosciences and Natural Resources (BGR), D-30655 Hannover, Germany

19 ⁹Université de Lorraine, AgroParisTech, INRAE, UMR Silva, 54000 Nancy, France

20 ¹⁰TU Braunschweig, IGÖ - Abt. Umweltgeochemie, 38106 Braunschweig, Germany

21

22 Corresponding Authors:

23 John D. Marshall john.marshall@gu.se

24 Matthias Beyer, matthias.beyer@tu-bs.de

25 **Abstract**

26 Water labeled with stable isotopes provides a conservative tracer, being neither produced nor
27 consumed, for water flowpaths within soils and root systems. We added a strong, evenly distributed
28 ²HHO label to one m² of soil surface and continuously monitored its passage downward into the soil
29 and upward into the stems of surrounding trees, with the objective of illuminating spatiotemporal
30 lateral root water uptake and overlap. The study was conducted during the historic drought of 2018 in
31 a mature Scots pine (*Pinus sylvestris*) forest growing on sandy soil in northern Sweden. Continuous
32 *in situ* isotopic measurements of tree xylem water evidenced root system overlap of six trees within



the labeled square meter, . This result is consistent with previous estimates from labelled nutrient uptake measurements at this site. However, label uptake differed sharply among trees, even within the same radius; 90% of the label was taken up by one of the two trees closest to the labelled plot. Horizontal transport rates in tree roots averaged $0.17 \pm 0.05 \text{ m d}^{-1}$, meaning that the arrival of label pulse in tree stems was delayed by 6-33 days from first tree to last. Root water uptake by trees appeared restricted to the upper 60 cm of mineral soil, even at the peak of the drought. Label intensity of the mineral soil weakened throughout the drought, consistent with the notion that the label was being dispersed or diluted. Labeled water recovery was low (3-4%), and we hypothesize that this was due to a significant upward flux of water into the organic surface horizons. Our data provide a daily and three-dimensional description of the passage of a labeled water pulse, highlighting the heterogeneity in horizontal water transport flowpaths and the uneven partitioning of label among individual trees in a boreal forest.

Introduction

Trees take up enormous quantities of water from the soil to grow and survive. This uptake is driven by atmospheric demand for water vapor (Campbell and Norman, 2012), and is constrained by soil moisture availability and root distributions (Bachofen et al., 2024; McCulloh et al., 2003). In forests, roots of different individuals, and their mycorrhizae, extend and overlap both vertically and horizontally, thus sampling across heterogeneous water availabilities (Bachofen et al., 2024; Goldsmith et al., 2019), while also competing for water and nutrients (Henriksson et al., 2021; Lutter et al., 2021). So far, vertical patterns of root water uptake have been studied more often than horizontal patterns (Beyer et al., 2016; Jackson et al., 1996; Stocker et al., 2023).

In one of the rare studies investigating horizontal uptake patterns in forests, uptake as far as 3-6 m from the stem was found (Sternberg et al., 2002; Sternberg et al., 2005). Whether vertical or horizontal, long-distance transport comes at a considerable carbon expense to the tree (Guswa, 2008), which must ultimately limit the benefits of long horizontal roots. The costs and benefits are complicated by the near universality of common mycorrhizal networks (Martin and van der Heijden, 2024; Simard and Durall, 2004), which could extend uptake zones beyond the range of individual root systems. At present, the physiological significance of these networks is insufficiently quantified (Henriksson et al., 2023; Martin and van der Heijden, 2024). Here, we use “root” water uptake as shorthand to refer to tree roots plus their mycorrhizal partners.

These observations raise questions about the degree of overlap in uptake zones between individual trees (Henriksson et al., 2021; Kulmatiski et al., 2020). One might argue that, at the extreme, there would be no root overlap and tree roots systems would grow as if each owned property, perhaps avoiding other roots when they were approached (Mahall and Callaway, 1992). On the other hand, roots might overlap extensively, making use of the limited space in their immediate vicinity, whether it is occupied by other roots or not. Most data suggest the latter (Kulmatiski et al., 2010; Lutter et al., 2021; Lwila et al., 2024), but there are instances of the “territoriality” implied by the former (Kuiper



71 and Coutts, 1992). Quantification of this overlap is needed for scaling water and nutrient uptake from
 72 individual trees to forest stands (Manoli et al., 2014), as well as for estimating belowground
 73 competition for studies of tree drought response, silviculture and production ecology (Lutter et al.,
 74 2021). Finally, the overlap might reveal novel underground ecological processes, for example water
 75 sharing among individuals (Kakouridis et al., 2022). Tracing water flowpaths within soils is
 76 challenging and involves destructive sampling, which implies large disturbances to the soil column
 77 and potentially irreversible harm to the root system. *In situ* methods based on online monitoring of
 78 soil and tree xylem water isotopic composition allow for tracking water through the soil-plant-
 79 atmospheric continuum in real time (Beyer et al. 2020). But so far, there have been few isotopic
 80 assessments of water uptake dynamics (Gessler et al., 2022; Kühnhammer et al., 2022, 2023;
 81 Landgraf et al., 2022; Seeger and Weiler, 2021; Volkmann et al., 2016).

82 We studied these questions in a boreal forest in northern Sweden during the “drought of the century”
 83 in the summer of 2018 (Gutierrez Lopez et al., 2021). This episode provided a unique condition
 84 wherein long horizontal or deep vertical roots might have been important, especially if they reached
 85 into distant water sources (Bachofen et al., 2024). Such a shift in water sources might (Lindroth et al.,
 86 2020) or might not (Gessler et al., 2022) compensate for soil drying, holding canopy
 87 evapotranspiration constant (Bachofen et al., 2024). Responses to this drought event have already
 88 been described elsewhere in terms of sap flow (Gutierrez Lopez et al., 2021), latent heat flux
 89 (Lindroth et al., 2020; Mensah et al., 2021), and vertical water uptake patterns (Gessler et al., 2022).
 90 Horizontal water uptake over the whole growing season was described in an earlier study at the same
 91 site (Henriksson et al., 2021), but the short-term dynamics during the peak of the drought and the
 92 recovery period have not been investigated previously.

93 Here, we monitored continuously and *in situ* soil and tree xylem water isotopic composition during
 94 the peak and drought recovery periods. This experiment followed the dynamics and spatial
 95 distributions of a point-labeling with ^2HHO in a mature pine forest, where considerable root
 96 interaction had previously been reported (Henriksson et al., 2021). We aimed to quantify the
 97 interaction using water uptake patterns among co-occurring tree individuals, to quantify rates of
 98 horizontal water transport through roots, and to describe the fate of a label applied to the surface of a
 99 deep sandy soil.

100 **Materials and Methods**

101 **2.1 Study site**

102 This study was conducted in a ~100-year-old naturally regenerated, homogeneous forest dominated
 103 by Scots pine (*Pinus sylvestris* L.), in northern Sweden (Rosinedalsheden, 64°10'N, 19° 45'E, 145 m
 104 a.s.l.). Understory vegetation was composed of ericaceous shrubs (*Vaccinium myrtillus* L. and
 105 *Vaccinium vitis-idaea* L.) and a layer of mosses and lichens. In 2013, the leaf area index was 2.7 m²m⁻²



106 ². The stand averaged 18.6 (sd = 0.1) cm in diameter and 17.5 (sd < 0.1 m) m in total height in 2013
 107 (Lim et al., 2015). The climate is typical of the northern boreal zone: average annual temperature and
 108 precipitation are 2.4 (sd = 0.8) °C and 638 (sd = 107) mm, respectively (Klosterhalfen et al., 2023).
 109 Winters are cold and long; summers are usually cool and wet. The photosynthetically active period
 110 extends from mid-April to mid-November (Tarvainen et al., 2018; Vernay et al., 2020). A soil
 111 description was performed at a nearby forest, approximately 6 km away, under similar stand and
 112 landscape conditions. The soil was labeled a Regosol (FAO 1988) that had formed on fluvial
 113 sediment. The texture was considered loamy sand to sandy loam with lenses of silt loam at 25–45 cm
 114 depth. The clay content was less than 11% (Plamboeck et al., 1999).

115 The sample plot was located approximately 30 m from an eddy covariance system installed on a
 116 tower above the uniform canopy (21.5 m above the ground) (Lindroth et al., 2020; Zhao et al.,
 117 2022). The eddy covariance system measured latent energy fluxes from the canopy over the whole
 118 study period using H₂O mixing ratios measured with a gas analyzer (LI-7200, LI-COR
 119 Environmental, Lincoln, USA) at 20 Hz frequency (Jocher et al., 2017).

120 The study was conducted from June to September 2018, when northern Scandinavia, like much of
 121 central Europe, underwent an exceptional drought; in Scandinavia, it was the driest period in fifty years
 122 (Gutierrez Lopez et al., 2021; Lindroth et al., 2020). From snowmelt (18 May) until 23 July, a period
 123 of more than two months, the study area received only 56 mm precipitation. The drought was then
 124 broken by a series of strong rainfall events that delivered 85 mm in eight days. We applied the soil label
 125 in the middle of the drought period and tracked its passage through the last two weeks of the drought
 126 and into the wetter period afterward.

127 **2.2. Continuous measurements of water isotopic composition**

128 *2.2.1. Experimental design*

129 We selected 15 Scots pines within a circular plot of 12 m radius around the labeled area (Fig. 1). To
 130 study horizontal transport of water, we applied isotopic tracer on 10th of July 2018 over a 1-m² area in
 131 the center of the experimental plot. We present the isotopic data in δ -notation (Gonfiantini, 1978), with
 132 units of per mil (‰) relative to the VSMOW-SLAP scale. The tracer consisted of a mixture of 25 L of
 133 deionized tap water ($\delta^2\text{H}$: -90‰) with 200 mL of ²H-enriched water (²H₂O, 99.5%), yielding a ²H
 134 atom fraction of 0.0163 ($\delta^2\text{H} \cong 106,000\text{‰}$). The ²H-enriched water was injected at the surface of the
 135 mineral soil (i.e., underneath the moss and humus layers) by forcing a rigid plastic tube through the
 136 organic layer and injecting water into the created hole using a syringe. To ensure homogeneous
 137 distribution of the tracer, we applied 70 mL at each of five points within each 12.5 × 12.5 cm grid across
 138 the 1-m² label area, totaling 320 injections (22.4 L). After injections on the grid were complete, we
 139 injected the small volume of remaining label randomly within the labeled area.



140 For the sake of completeness, it should be noted that two additional labeling experiments were
 141 attempted. The first, on the 6th of June, 2018 (soon after snowmelt), consisted of applying a weaker
 142 ($\delta^2\text{H} = 3500\text{‰}$) label to the same 1-m² plot. The label was briefly detected in the surface soils but did
 143 not show up in the trees at all. Therefore, we repeated the labeling with the stronger ($\delta^2\text{H} \cong 106,000\text{‰}$)
 144 label solution described above, on July 10th. The second experiment, on the 20th of July 2018, was
 145 designed to detect deep water uptake (Burgess et al., 1998; Caldwell and Richards, 1989; Dawson and
 146 Pate, 1996; Moreira et al., 2000). We applied 1 L of deionized water containing 2.94 mL of H₂¹⁸O ($\delta^{18}\text{O}$
 147 $\cong 470\text{‰}$), at a depth of 50 cm, directly under the stems of five trees (see Beyer *et al.*, (2016, 2018) for
 148 further application details). We did not detect the ¹⁸O label in any of these trees (data not shown).
 149 However, to avoid potential interferences between labeling experiments, these trees were dropped from
 150 consideration. They are represented by purple symbols in Figure 1 and not addressed further.

151 2.3 Volumetric water content

152 Volumetric soil water content (VWC) was measured along a vertical profile inside the labeled area
 153 using TDR probes (5TM, Metergroup, Pullman, USA). The TDR probes were placed at 10, 30, 50, 70,
 154 and 100 cm soil depth. For our sandy soils, we used the factory-default calibration. We took particular
 155 care when installing both the TDR and the isotope probes (see 2.3.2) to avoid damaging roots during
 156 probe installation, hoping that the roots from all surrounding trees would continue to take up water
 157 normally from the labeled block of soil. We estimated total water uptake by measuring the daily decline
 158 in VWC at each depth, multiplying VWC by the soil depth represented by that sample, and
 159 accumulating the decline over all depths (the single-step, multi-layer water balance of Guderle and
 160 Hildebrandt, 2015):

$$161 \quad \Sigma U = \Sigma (\Delta \text{VWC}_{10} * D_{10} + \Delta \text{VWC}_{30} * D_{30} + \Delta \text{VWC}_{50} * D_{50}) \quad \text{Eq. 1}$$

162 Where UD is mean uptake depth per day, ΔVWC_n is the daily change in VWC at depth n , D_n is the
 163 thickness of the layer represented by each VWC (always 20 cm). We then measured the mean depth of
 164 uptake was by weighting $\Delta \text{VWC}_n * D_n$ of each layer by its mean depth, summing, and dividing by the
 165 total uptake, thus:

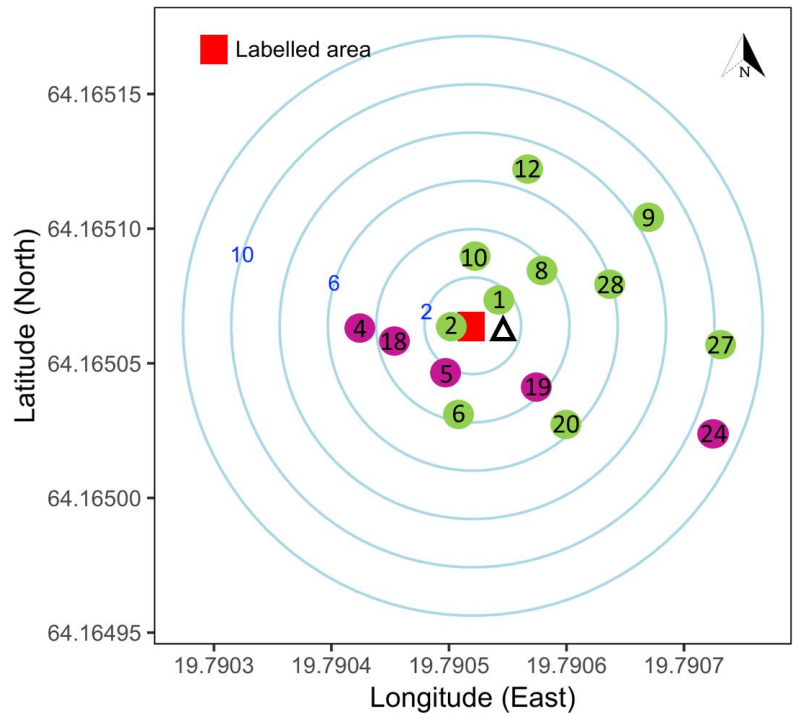
$$166 \quad \text{UD} = \Sigma (\Delta \text{VWC}_{10} * D_{10} * 10 + \Delta \text{VWC}_{30} * D_{30} * 30 + \Delta \text{VWC}_{50} * D_{50} * 50) / \Sigma U \quad \text{Eq. 2}$$

167 Where UD is mean uptake depth and 10, 30, 50 cm are the depths of each VWC sensor. ΣU

168 is the sum of uptake (Eq. 1).

169 This approach yields a water consumption rate (ΣU) in cm day⁻¹, integrated over the upper 60 cm of
 170 mineral soil. Because the uppermost TDR probe was 10 cm deep in the mineral soil and covered by the
 171 forest floor, we assumed there would be little contribution of soil surface evaporation to this flux.

172



173

174 *Fig. 1. Map of studied trees (filled circles). The 1-m² plot labeled with ²H₂O is shown in the center as a red square.*
175 *The trees labeled with H₂¹⁸O and subsequently dropped from the study are shown in purple. Two Picarro L2130i*
176 *analyzers were placed in a box at the triangle. Horizontal distance from the center of the labeled plot is indicated*
177 *by the blue concentric rings and blue numbers. Distances of individual trees from the plot center are presented in*
178 *Table S1.*

179

180 2.3.2. In situ measurements of the soil and plant water isotopic composition

181 From June to September 2018, we measured the stable isotopic composition ($\delta^2\text{H}$ and $\delta^{18}\text{O}$) and soil
182 VWC across depth inside the 1m² plot. The isotopic composition was measured with custom-made
183 equilibration probes inserted at depths of 5, 10, 15, 20, 30, 50, 70, and 100 cm depth in the center of the
184 labeled soil volume. The probes consisted of two PFA Teflon tubes (1/8"AD, 1/16" ID, Teddington
185 AB, Skogås, Sweden) that were glued (Pattex Kraft-Mix, Henkel AG & Co. KGaA, Düsseldorf,
186 Germany) into a gas-permeable membrane (Accurel GP V8/2HF, 3 M, Germany; 0.155 cm wall
187 thickness, 0.55 cm i.d., 0.86 cm o.d.) of 10 cm length. One of the two Teflon tubes was inserted a short
188 distance into the probe. It provided air drawn through a desiccant tower (Drierite, Hammond, Xenia,
189 OH, USA) reducing potential contamination with ambient water vapor. The second tube was placed at
190 the opposite end of the probe to ensure that the air stream would equilibrate isotopically with soil water



191 before leaving the probe. This tube was connected to a Picarro 16-port distribution manifold (A0311,
 192 Picarro Inc., Santa Clara, USA). The manifold was connected to a Picarro L2130i CRDS (Cavity Ring-
 193 Down Spectroscopy) water isotope analyzer. We verified that materials used did not affect measured
 194 isotopic composition by placing them in ambient air and comparing to measurements without soil
 195 probes. To prevent condensation, the PFA tubes were heated by electrical heating lines (TE's Raychem,
 196 TE Connectivity, Schaffhausen, Switzerland) wrapped in foam insulation tubes (Armacell, Münster,
 197 Germany).

198 We also measured the isotopic composition of tree xylem using the borehole equilibration method
 199 (Marshall et al., 2020). To measure xylem $\delta^2\text{H}$ and $\delta^{18}\text{O}$, a borehole was drilled all the way through the
 200 center of each tree. All trees were cored along the N-S axis at a height of 1.3 m using an electric drill
 201 with a 5-mm bit. We rinsed the boreholes with acetone to avoid the obstruction of cells by pitch
 202 (Marshall et al. 2020). One end of the borehole was open to the atmosphere to allow equilibration of
 203 ambient water vapor with liquid xylem water evaporated inside the borehole. We have previously
 204 shown that equilibration occurs even if ambient water vapor is added at the borehole inlet (Marshall et
 205 al., 2020). The other end of the borehole was coupled to 6-mm PFA tube (Teddington AB, Skogås,
 206 Sweden) using stainless steel connectors (Swagelok) plumbed to a rotary 16-port valve (Vici, Valco
 207 Europe, Schenk, Switzerland). The valve was connected to a second Picarro L2130i CRDS water
 208 isotope analyzer. Again, electrical heating lines wrapped in foam insulation pipes were installed to
 209 prevent condensation in the PFA tubing and the valve. This setup allowed continuous measurements of
 210 water concentration and isotopic composition of the water vapor equilibrated inside the borehole and
 211 allowed us to calculate the isotopic composition of the xylem water (Marshall et al., 2020).

212 All trees and the water isotope values of the atmosphere were monitored sequentially. Automatic
 213 calibration of the analyzer was performed every five hours using the Picarro Standard Delivery Module
 214 (SDM). The SDM injects a water standard of known isotopic composition into the analyzer's vaporizer.
 215 Each of the standards was measured in vapor phase for 20 minutes at two flow rates: $0.08 \mu\text{L s}^{-1}$ and
 216 $0.05 \mu\text{L s}^{-1}$. The two injection rates produced different water vapor concentrations, which we used to
 217 correct for the concentration-dependence of the isotope measurements. At each injection rate, we used
 218 two standards covering the range of expected variability in $\delta^2\text{H}$ and $\delta^{18}\text{O}$: depleted deionized water ($\delta^2\text{H}$
 219 = -94.28 ‰ and $\delta^{18}\text{O}$ = -12.87 ‰) and a homemade $\delta^2\text{H}$ -enriched standard ($\delta^2\text{H}$ = 225.8 ‰ , $\delta^{18}\text{O}$ = $-$
 220 12.70 ‰). Any drift in instrument readings would have been detected and corrected for the multiple
 221 calibrations within each day. The isotopic composition of the two standards was determined on an
 222 isotope ratio mass spectrometer (DeltaV, Thermo Fisher) at the Stable Isotope Laboratory of the
 223 Swedish University of Agricultural Science (Umeå, Sweden). Each tree was measured for at least 30
 224 minutes and the duration of the measurement interval for each tree was adjusted depending on the tube
 225 length. To avoid memory effects when the valve had just turned, we used only the data from the last
 226 five minutes in each valve position. To further avoid non-steady state conditions, as when condensation



may have been present or stem temperatures were rapidly changing, we deleted values of water concentration with a standard deviation higher than $1,000 \mu\text{mol mol}^{-1}$ or values of water concentration that were higher than $50,000 \mu\text{mol mol}^{-1}$.

Borehole temperature is a critical parameter for calculating xylem isotopic composition because it is needed for the conversion of water isotope values in measured vapor phase to liquid xylem water (Eq. 1-3). Copper-constantan thermocouples (Omega Engineering, Norwalk, CT, USA) were installed at approximately 2 cm depth within the borehole and in contact with the surface of the xylem tissue to measure the temperature of the xylem surface. We further filtered all data for which difference in temperature between the borehole and the atmosphere was higher than 5 degrees, which occurred most often when the temperature was rapidly changing in the morning and evening. As above, this was done to reduce the effects of condensation within the borehole or the tubing and to avoid the risk of non-steady state temperatures conditions within the borehole.

2.4 Data processing and analyses

2.4.1 Calculation of $\delta^2\text{H}$ and $\delta^{18}\text{O}$ of xylem water

After calibration and instrument drift-correction, the xylem liquid water $\delta^{18}\text{O}$ and $\delta^2\text{H}$ values were estimated using the relations proposed by Majoube (1971) for describing the equilibrium fractionation between the liquid and vapor phases of $\delta^2\text{H}$ and $\delta^{18}\text{O}$ based on the temperature (T in K) measured by the thermocouples in the borehole:

$$1000 \ln \ln \alpha_{2\text{H}} = \frac{24.844 \times 10^6}{T^2(\text{K})} - \frac{76.248 \times 10^3}{T(\text{K})} + 52.612 \quad \text{Eq. 3}$$

$$1000 \ln \ln \alpha_{18\text{O}} = \frac{1.137 \times 10^6}{T^2(\text{K})} \quad \text{Eq. 4}$$

The resulting α -values were multiplied by the raw isotope ratios (R, e.g., $^2\text{H}/^1\text{H}$) of equilibrated water vapor ($R_{2\text{Hvap}}$) to estimate liquid water isotopic ratio ($R_{2\text{Hliq}}$):

$$R_{2\text{Hliq}} = R_{2\text{Hvap}} * \alpha^2\text{H} \quad \text{Eq. 5}$$

They were then converted back to delta notation.

The soil liquid water values were estimated using a “regression” method that uses a polynomial calibration curve to simultaneously account for isotopic equilibration (Majoube, 1971), device-specific effects of water vapor concentration, and the interaction of the sampling probe with the soil (Beyer et al., 2018, 2020; Oerter and Bowen, 2017). Regressions were fitted to measurements of dried bulk soil from the field site, placed in impermeable bags and filled with liquid water of known isotopic composition (“standards”). As with the xylem, these calibration measurements were made each time



the manifold cycled through the samples throughout the field campaign. The resulting regression equations were:

$$^2H_{liquid} = (2.631e-04 * ^2H_{vapor})^2 + 1.216 * ^2H_{vapor} - 0.001379 * H_2O + 119.9 \quad Eq. 6$$

with adjusted $R^2 = 0.9987$, and:

$$^{18}O_{liquid} = (-6.318e-09 * H_2O)^2 + 0.7895 * ^{18}O_{vapor} + 0.00005189 * H_2O + 5.754 \quad Eq. 7$$

with adjusted $R^2 = 0.85$.

2.4.2 Calculation of line-conditioned excess

To detect subtle increases in the δ^2H -enriched water in the trees, we used the local meteoric water line to calculate line-conditioned deuterium-excess (lc-excess) (Landwehr and Coplen, 2006). The local meteoric water line was estimated from precipitation collected at the Svartberget field station (<https://www.icos-sweden.se/Svartberget>), 8 km away. There were 225 samples collected at least biweekly during the whole of 2017 and 2018. The resulting LMWL was:

$$\delta^2H = 1.32 + 7.44 * \delta^{18}O \quad Eq. 8$$

with $R^2 = 0.97$.

The lc-excess was then calculated as:

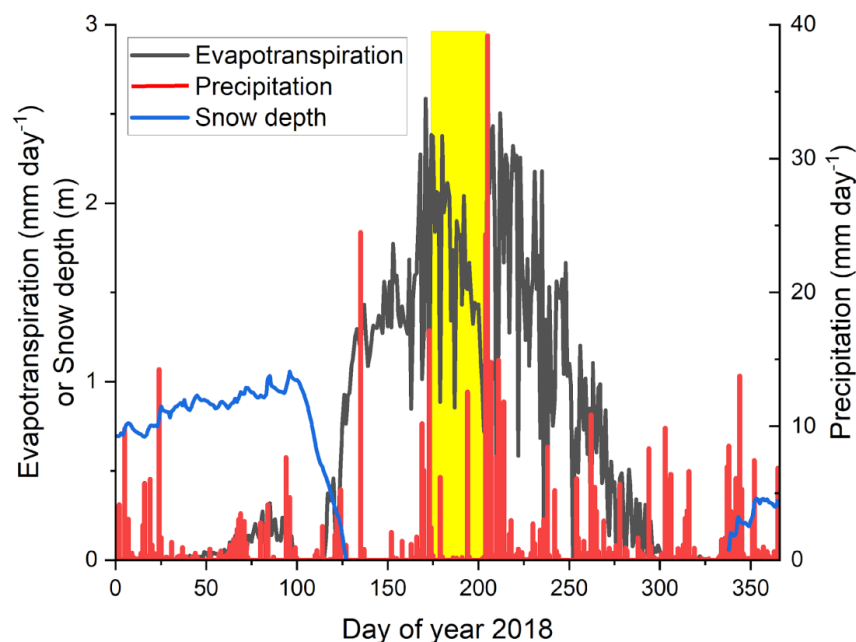
$$lc-excess = \delta^2H_{measured} - (1.32 + 7.44 * \delta^{18}O_{measured}) \quad Eq. 9$$

Values of lc-excess above zero were interpreted as evidence of the uptake of δ^2H -enriched water. The advantage of this approach is that it removes background variation in δ^2H that is correlated with $\delta^{18}O$, revealing low levels of labeling more clearly than the raw isotopic compositions. All analyses were performed using either excel or the base package of R (R Core Team (2023)).

3 Results



285 The summer of 2018 began with only one significant rainfall after the snowpack melted. During the
 286 drought that followed, ecosystem evapotranspiration fell by about 50% but recovered immediately after
 287 the first rains (Fig. 2).



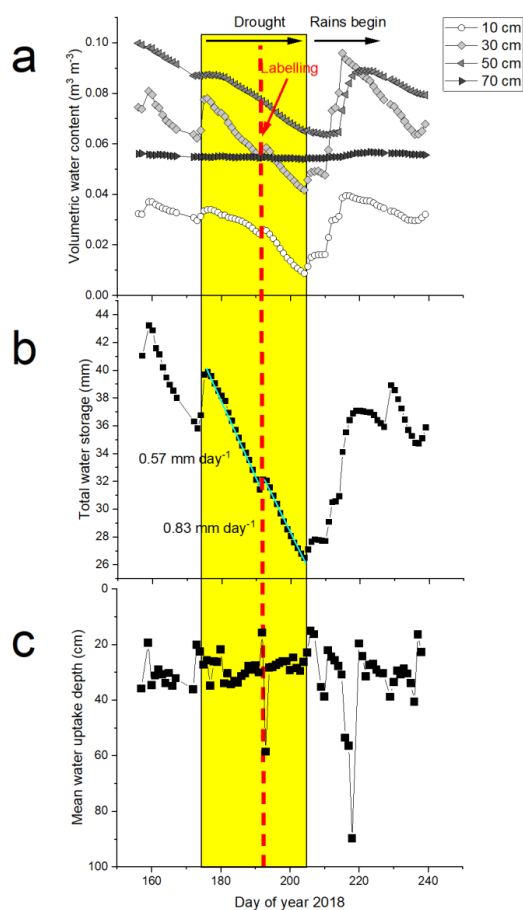
288

289 *Fig. 2. Daily evapotranspiration at the Rosinedalheden boreal pine forest in calendar year 2018. The*
 290 *yellow box highlights the period of the drought. The drought began on day 174, more than a month*
 291 *after the snowpack melted (blue line), and was interrupted by only one small precipitation event (red*
 292 *bars). The drought ended with a series of large events beginning on day 204.*

293 During the drought, the VWC fell at all depths within the upper 50 cm of soil (Fig. 3a). In contrast,
 294 the 70-cm depth showed almost no variation in VWC, consistent with our visual observations that
 295 there were few roots there. The isotopic labeling, which amounted to 25 mm of water on this plot,
 296 occurred on DOY 191, and was accompanied by small, short-lived increases in VWC at 10 and 30
 297 cm. The depth-weighted VWC in the upper 60 cm of soil (Fig. 3b) declined by 0.57 mm day⁻¹ in the
 298 early part of the drought and 0.83 mm day⁻¹ during the latter part (both R²>0.99). Mean water uptake
 299 depth (Fig. 3c) reflected the steep decline at 30 cm depth, averaging approximately 30 cm throughout
 300 the drought. Brief excursions were detected after the water additions due to labeling (DOY 191) and
 301 the first rains (DOY 203). In general, mean water uptake depth moved towards the surface during the



302 drying event. After the rains began on DOY 203, VWC sharply increased at all depths down to 50
 303 cm, with the sharpest increase detected at 30 cm.
 304
 305



306
 307

308 *Fig. 3. a) Soil VWC (VWC) by depth under the labeled 1-m² area; b) Total water storage summed*
 309 *over 60 cm of soil depth. Slopes of regression lines were fitted to the drought-induced decline,*
 310 *neglecting the day after the labeling (m); c) Mean daily water uptake depth. The strong positive*



excursions are associated with labeling and rainfall events. In all panels, the drought period is shown by the yellow box and the labeling date is shown as a vertical, dashed red line at DOY 191.

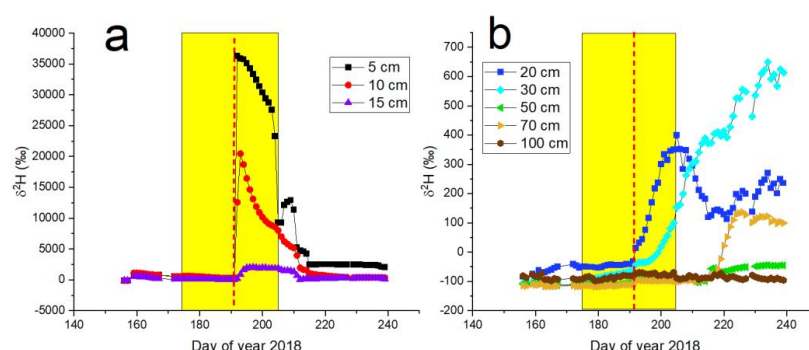
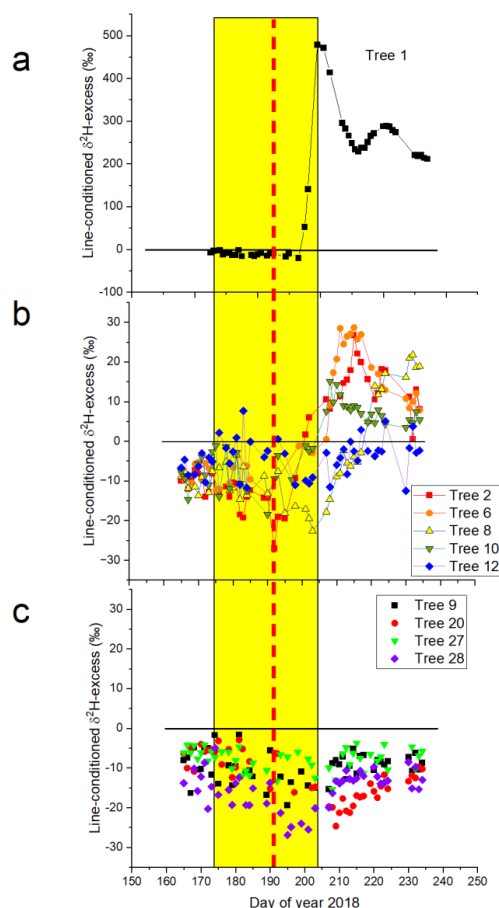


Fig. 4. Isotopic composition (δ^2H) of soil water by depth showing a) δ^2H of depths up to 15 cm, b) δ^2H of depths 20 cm and below. Note the differences in y-axis scaling. . In both panels, the drought period is shown by the yellow box and the labelling date is shown as a vertical, dashed red line at DOY 191.

After the 2HHO labeling, the isotopic signature observed in the 5-cm probe briefly rose above 35,000 ‰, in the 10-cm probe above 20,000 ‰, and in the 15-cm probe above 2,000‰ (Fig. 4a). The probes at 20, 30, 50, and 70 cm responded more slowly and less strongly (Fig. 4b). We detected no increase in δ^2H at 100 cm depth by the end of August (DOY 240). Thus the label was concentrated in the upper 10-15 cm, especially in the period immediately after the labeling. In these upper depths, the label intensity fell by around 1,000 ‰ day⁻¹ over the drought period and then dropped sharply when the rains arrived on day 204. Below, label intensity increased at 20 and 30 cm even before the rains arrived. The probe at 50 cm detected the label weakly, but the 70 cm probe detected it clearly; both the 50- and 70-cm probes responded about four weeks after the labeling. The $\delta^{18}O$ also increased at 5 and 10 cm after the 2HHO labeling, but the increase was at most ≈ 20 ‰ (Fig. S1), three orders of magnitude smaller than for δ^2H (Fig. 4a).



333

334 *Fig. 5. Line-conditioned deuterium-excess (lc-excess) of xylem water in tree stems. Values above zero,*
 335 *denoted by the horizontal black line, show likely label uptake. Panel a) Tree 1, near the soil-labeling*
 336 *plot; b) Labeled trees with lc-excess at some point greater than zero; c) Unlabeled trees, all more*
 337 *than 4 m from the center of the labeling plot. Note that the y-axes are on different scales and the zero-*
 338 *intercepts are at different locations on panel a vs panels b and c. In all panels, the drought period is*
 339 *shown by the yellow box and the labelling date is shown as a vertical, dashed red line at DOY 191.*

340 Among the trees surrounding the 1-m² label plot, we detected the label in six (i.e. lc-excess > 0). Tree
 341 1 showed by far the highest $\delta^2\text{H}$ values (Fig. 5a) and was responsible for 90% of the cumulative label
 342 water uptake in the study (Fig. S2). The $\delta^2\text{H}$ of the xylem sap of this tree (at 1.3 m height) began to
 343 change about four days after labeling and it reached its maximum (nearly 500 ‰) eight days after the
 344 labeling (Fig. 5a). The label intensity then decreased, maintaining relatively high enrichment until the
 345 end of the experiment. In contrast, $\delta^{18}\text{O}$ of this tree displayed only a slight increase (≈ 2 ‰) during



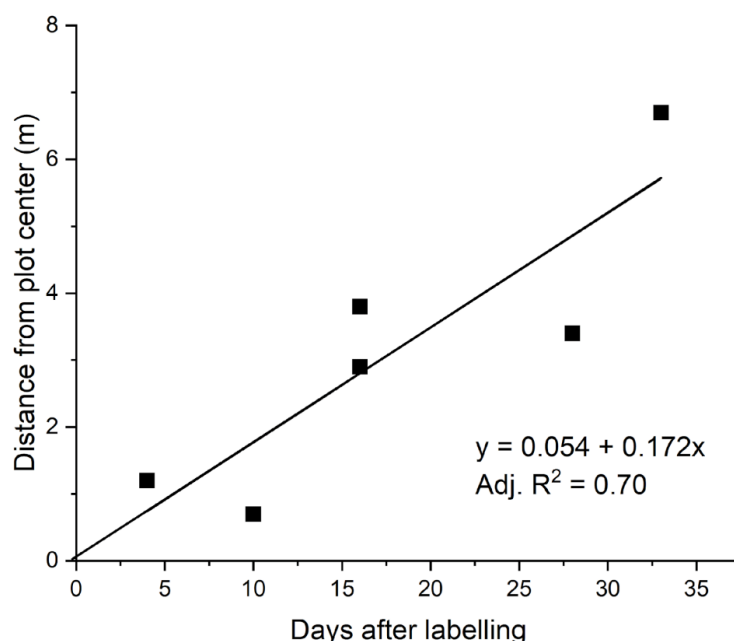
346 this period (Fig. S3). Four other trees on the plot increased $\delta^2\text{H}$ steadily over about two weeks after
 347 the labelling (Fig. 5b) reaching lc-excess values greater than zero. All these trees were within 4 m of
 348 the plot center. Three of the four trees within the 4-m radius began to respond before the rains started.
 349 Although it was more than 4 m from the plot center, Tree 12 also displayed lc-excess values greater
 350 than zero, but only briefly (Fig. 5b). The other trees that were more than 4 m from the plot center
 351 showed no response to the labeling (Fig. 5c).

352

353

354

355



356

357 *Figure 6. Distance from the plot center vs. number of days after labelling. Only trees that responded*
 358 *to the labeling are shown.*

359 Among the six trees that showed label uptake, the breakthrough time varied with distance (Fig. 6).

360 The first tree (Tree 1, 1.2 m from plot center, Table S1) required four days for label arrival and the

361 last (Tree 12, 6.7 m from plot center) required 33 days. The x-intercept was approximately equal to



the label date (0 on this x-axis) and the slope of the regression line ($0.172 (0.05) \text{ m day}^{-1}$) described the maximum horizontal transport rate.

4 Discussion

We added a strong $\delta^2\text{H}$ -labeled water pulse to 1 m^2 of the mineral soil surface in a mature boreal Scots pine forest and monitored water isotopic composition in soils and tree xylem continuously afterward. The label initially remained near the soil surface, but it gradually moved deeper into the soil and was eventually detected as deep as 70 cm. The label was also taken up by roots, as evidenced by the label presence in xylem water of six surrounding trees, including all trees within 4 m of the labeled plot center. The labeling occurred during a drought of rare intensity in the boreal north. We were able to observe labeling patterns both during the drought and after the rainfall events that relieved it.

Horizontal transport and xylem water isotope dynamics

The experiment was designed primarily to detect and quantify patterns of root (and mycorrhizal) overlap and dynamics of horizontal water uptake by trees. We found the label in stems of six surrounding trees. We therefore conclude that all of these trees had roots in the labeled 1-m^2 plot. This is far more overlap than we observed in the crowns, which scarcely overlap at all in the horizontal direction.

There are relatively few studies describing horizontal water uptake patterns in forest trees (Göttlicher et al., 2008; Henriksson et al., 2021; Lutter et al., 2021). Root distributions have been mapped in some temperate forests (Gao et al., 2021; Kuiper and Coutts, 1992; Lwila et al., 2024), but the presence of roots is not sufficient to predict water uptake (Göttlicher et al., 2008). Long-distance horizontal transport through overlapping root systems might increase uniformity in water availability among trees. It might also favour trees near openings by providing access to the unused soil water in the openings (Lutter et al., 2021; Moreira et al., 2000; Sternberg et al., 2002; Sternberg et al., 2005). This favouring might, as with deep vertical roots, provide a “lifeline” to trees growing under extreme drought conditions (Bachofen et al., 2024). However, it might also represent a significant carbon cost (Guswa, 2008), perhaps reducing partitioning to aboveground production (Fernandez-Tschieder et al., 2024; Marshall et al., 2023).

The rate of uptake varied among tree individuals. For example, the stem of Tree 2 was at the edge of the labeled plot (0.7 m from the center of the plot) and yet it showed far less label than Tree 1, which was slightly farther away (Figs. 5a and 5b). The label intensity detected in tree xylem became rather weak with greater distance from the plot, which we addressed by calculating the $1c\text{-excess}$. This parameter corrected for event-based variation using the strong correlation between natural abundance of $\delta^2\text{H}$ and $\delta^{18}\text{O}$, allowing us to detect low levels of labeling. When we focused simply on the first



396 appearance of the label, as defined by lc_{excess} greater than zero, we found that there was a
 397 correlation with distance from the plot (Fig. 6), suggesting that the label took some time to traverse
 398 the horizontal distance to the stems. The slope of this relationship, $0.17 (0.05) \text{ m day}^{-1}$, is an estimate
 399 of the maximum horizontal transport rate. For comparison, measurements of water flow through pine
 400 stems are typically around 1 m day^{-1} (Plamboeck et al., 1999; Tarvainen et al., 2018). Note also that
 401 the label appeared in Tree 1 in only four days. This suggests that the surface roots were alive and
 402 ready to begin water uptake, despite the severe drought (Marshall, 1986). The peak label intensity in
 403 Tree 1 appeared eight days after the labeling, perhaps due to the arrival of label via slower flow paths
 404 after its initial breakthrough (Gao et al., 2021; Seeger and Weiler, 2021; Werner et al., 2021).
 405 Alternatively, as the drought advanced, the tree could have increased the amount of water taken up
 406 from deeper soil layers (e.g., Gessler et al. 2022); however, our VWC data suggest that deep water
 407 uptake did not increase as a proportion of the total (Fig. 3c) late in the drought.

408 We also observed a brief, weak pulse in $\delta^{18}\text{O}$ of the surface soil horizons after the labeling. This
 409 might have occurred due to $\delta^{18}\text{O}$ -enrichment of the $^2\text{H}_2\text{O}$ used for labeling (not measured), but we
 410 believe it is more likely interference in the spectrometer by the strong $^2\text{H}^1\text{H}^{16}\text{O}$ absorption peak with
 411 the adjacent $^1\text{H}^1\text{H}^{18}\text{O}$ peak, which has been observed in other studies using high concentrations of $\delta^2\text{H}$
 412 (Beyer et al., 2016, 2018). In any case, the apparent $\delta^{18}\text{O}$ pulse was orders of magnitude weaker than
 413 the $\delta^2\text{H}$ pulse and can be considered negligible.

414 *Ownership hypothesis*

415 The benefits of long horizontal roots could be assessed not only by the detection of label in
 416 surrounding trees, but also by the label intensity. One can imagine a continuum between complete
 417 domination of uptake by a single tree, analogous to owned and defended property, vs. complete
 418 sharing of the benefit, perhaps modified by radial distance from the tree stem. Although six trees were
 419 labeled, we detected a strong preference for uptake by one of the two trees nearest the plot center,
 420 while the other nearest tree took up very little of the label. This preference remained remarkably
 421 constant even as the label pulse dissipated (Fig. S2). These results are similar to the cumulative ^2HHO
 422 labeling observed in tree rings of trees in a replicated experiment at the same site, also conducted in
 423 2018. In order to investigate this “ownership hypothesis” further, we have used the data from this
 424 earlier experiment to rank the trees from each of their plots according to label intensity (Henriksson et
 425 al., 2021) (Fig. 7). Such a ranking shows a strong preference for the labeling of one or two trees, with
 426 much lighter labeling in several more (Fig. 7b). Henriksson et al., (2021) found that the most heavily
 427 labeled trees were not necessarily those nearest the labeled plot. We interpret these and our results as
 428 evidence of dominance, but not to the point of exclusion, leaning toward the defended property end of
 429 the water-sharing continuum introduced above. The trunk boreholes in our study were oriented north-
 430 south while the boreholes in Henriksson et al. (2021) were oriented toward the plot center. We



initially believed that borehole orientation would not matter because an earlier report had shown that label was evenly distributed throughout the tree circumference rather quickly in white pine (White et al., 1985). More recent evidence from our site (Tarvainen et al., 2018) suggests that this is not true. Our fixed borehole orientation (N-S) may have contributed to the weak labeling observed for Tree 2 (on the western edge of the labeled plot) compared to Tree 1 (to the northeast). We recommend orienting boreholes toward the labelling plot in future work studying horizontal water uptake patterns. However, even if the label intensity was weakened by the borehole orientation, the timing and magnitude of the label pulse among trees is interpretable based on the uniform timing (Figs. 5a, 5b) and distance effects (Fig. 6) in the trees where label was detected.

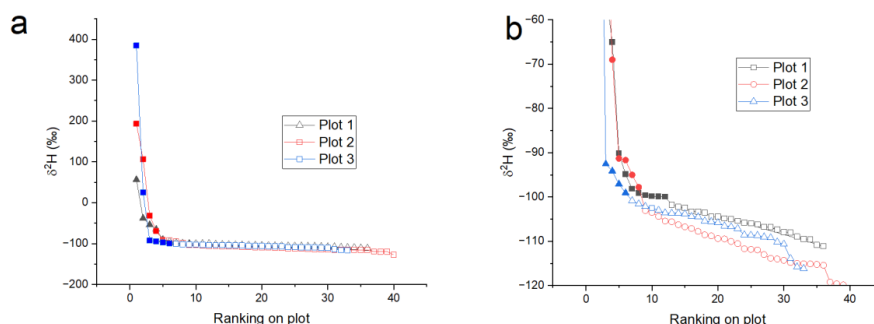


Fig. 7. Water isotopic composition (δ^2H) of xylem wood in trees surrounding three labelled 1-m² plots (data reprinted with permission from Henriksson et al., 2021). The trees surrounding each plot are ranked according to labeling intensity. Filled symbols represent trees that were identified as “labeled.” Panel a) shows the full data range and panel b) highlights the transition from lightly labelled to unlabelled trees.

Soil water content and vertical root water uptake

We interpret daily declines in soil VWC during the drought period as evidence of tree root water uptake throughout the upper 50 cm of mineral soil (Fig. 3a). The slopes of the declines at 10 and 50 cm are similar, but that at 30 cm is steeper. There was no evidence of change in water content at 70 cm, consistent with our informal observation that roots were rare below 50 cm depth. The integrated water loss rate averaged 0.057 cm day⁻¹ in the early part of the drought and increased to 0.083 cm day⁻¹



¹ in the last part, meaning that water uptake from these depths increased slightly as the drought proceeded. However, this conclusion is based on only three measurements across depth, the uppermost at 10 cm. The current study is similar to the classic study of Plamboeck et al. (1999), which was conducted at a nearby site with similar soils. Plamboeck et al. (1999) estimated that, without irrigation, the 2-cm humus layer provided 10% of total uptake in July. When we estimated the mean depth of water uptake (Fig. 3c), it was remarkably stable throughout this severe drought, with a slight upward shift toward the end. Our estimated mean uptake depth (30.6 (1.2) cm) was similar to a depth-weighted estimate based on Plamboeck et al.'s (1999) isotopic data (30.3 (0.07) cm). Both our results and those of Plamboeck et al. (1999) suggest a rather constant water uptake depth as a drought develops. This differs from a global meta-analysis, which found a downward shift in response to drought (Bachofen et al., 2024). If our trees cannot shift deeper under drought, then it may make the broad horizontal root distribution even more important as an emergency source of soil water.

Label Recovery

We used both VWC and lc-excess to estimate recovery of the labeled water pulse. The integrated VWC increased by 0.72 mm after the addition of 25 mm labeled water, representing 3% of the water volume added. The excess ²H represented 16.2 μm (16.2 mL) immediately after the label addition. This value is about 4% of the 400 mL ²HHO that was added to the plot. The close agreement between these percentages is encouraging, but their small magnitude highlights our inability to close the water budgets.

We speculate that the low recoveries are due to water absorption and root water uptake by the desiccated soil, tree roots, and understorey vegetation roots in the layers above our uppermost probe (5 and 10 cm below the surface of the mineral soil for δ^2H and VWC, respectively). For illustration, using the maximum VWC measured by Plamboeck et al. (1999) on a nearby site with similar soils and vegetation, we estimate that the humus layer could retain 6 mm of precipitation, the 0-10 cm mineral horizon could retain 20 mm more. Thus, added together, these two layers could have effectively retained all the water we added. The large rainfall event that broke the drought (37.2 mm) resulted in an increase of only 2.8 mm in total water storage (as in Fig. 3b), approximately 8% of the expected value. If 30% were lost to interception, then 26 mm fell to the soil. This would mean that ground vegetation, roots, litter, and upper 5 cm of soil retained 26-2.8 = 23.2 mm of precipitation, which is slightly less than the 25 mm we added as label and would have only allowed a small proportion of the label to reach our probes. Our choice to inject the label at the mineral soil surface ensured that we detected some of the label in the mineral soil, but it appears it was impacted by significant losses to the upper mineral and the organic layers as well.

Simplified borehole method



489 The method used to measure xylem water here included several simplifications of the borehole
 490 method used in previous studies. In particular, we did not use dry air (e.g., Kühnhammer et al., 2022)
 491 relying instead on the two-way exchange and equilibration of water vapor during the borehole passage
 492 (Marshall et al., 2020). In addition, we relied on the pump within the analyser to draw air through the
 493 boreholes under negative pressure, apparently without significant leakage into the downstream
 494 airflows. This eliminates the need for the upstream pump used in some other applications (e.g.,
 495 Kühnhammer et al., 2022). Finally, we did not use any screening material to inhibit microbial growth
 496 (Landgraf et al., 2022), relying instead on the natural defensive compartmentation of the xylem to
 497 serve that purpose (Shigo, 1984). Although a visible band of brown tissue formed around the
 498 borehole, our data showed that the borehole vapor continued to respond to xylem-water changes until
 499 the end of the experiment, more than three months after the boreholes were drilled. One complication
 500 that remained was the placement of an analyzer in the field. Several recent papers describe methods
 501 for field sampling and storage of water vapor for stable isotope analysis (Havranek et al., 2020;
 502 Herbstritt et al., 2023; Magh et al., 2022), which would mean sacrificing the continuous data streams
 503 collected here, but would circumvent the need for an analyzer in the field and provide opportunities
 504 for more replication.

505 These results provide a dynamic description of soil water storage, transport, and root water uptake,
 506 including passage of the label through surrounding tree stems as they take up the label for
 507 transpiration. The timing and detection of the label are consistent with expectations insofar as it
 508 supports the notion that the root systems of several trees overlap on each square meter of ground
 509 surface. However, the concentration of the label in a single tree was inconsistent with the notion of
 510 extensive horizontal sharing. This question deserves more attention as it influences the scaling of
 511 transpiration from trees to stands.

512 Author contributions: JM, MD, and MB conceptualized the work. MB and JM managed data curation
 513 and analysis. Funding support was organized by MB and MD. Methodology was organized by MB,
 514 DD, PK, KK, MC, and JM. JM wrote the initial draft, but all authors contributed to writing and
 515 visualization.

516 Acknowledgments:

517 We thank Noelia Saavedra, Nils Henriksson, and Hyungwoo Lim (SLU-Umeå) for their help with the
 518 labeling and measurement of these plots, and Nils Henriksson for permission to reanalyze his
 519 published data. Tomas Lundmark and the Svartberget Field Station of SITES provided housing for the
 520 group during the most intense part of this fieldwork. Tomas also provided the Picarro analyzer that we
 521 used for the tree measurements. We are also grateful to the Svartberget field staff for provision of the
 522 eddy covariance and meteorological data. Hector Correia (TU-Braunschweig) helped with the field
 523 work. RKM acknowledges the funding bodies Knut and Alice Wallenberg foundation within the



524 project Future Forests KAW 2018.0259. She was also financially supported by the AquaDiva CRC
 525 1076 within the project B02. MD was supported by DFG MD1688/1-1 and 6-1. TEG received funding
 526 from the Spanish Ministry of Science and Universities (MCIN/AEI/10.13039/501100011033/
 527 projects: CNS2024-154609 and RYC2021-031759-I) and from the Catalan Government (SGR-Cat
 528 2021 00849). KK was financially supported by the Volkswagen Foundation (contract no. [A122505](#);
 529 reference no. 92889 to MB) and the German Research Foundation (DFG, SFB 1537 ECOSENSE).
 530 MC acknowledges support from a grant by
 531 the French National Research Agency (ANR, ANR-21-CE02-0033-01) and from a grant overseen by
 532 ANR as part of the “Investissements d’Avenir” program (ANR-11-LABX-0002-01, Lab of
 533 Excellence ARBRE).

534

535

536 **References:**

- 537 Bachofen, C., Tumber-Dávila, S. J., Mackay, D. S., McDowell, N. G., Carminati, A., Klein, T.,
 538 Stocker, B. D., Mencuccini, M., and Grossiord, C.: Tree water uptake patterns across the globe, *New*
 539 *Phytol.*, 242, 1891–1910, <https://doi.org/10.1111/nph.19762>, 2024.
- 540 Beyer, M., Koeniger, P., Gaj, M., Hamutoko, J. T., Wanke, H., and Himmelsbach, T.: A deuterium-
 541 based labeling technique for the investigation of rooting depths, water uptake dynamics and
 542 unsaturated zone water transport in semiarid environments, *J. Hydrol.*, 533, 627–643,
 543 <https://doi.org/10.1016/j.jhydrol.2015.12.037>, 2016.
- 544 Beyer, M., Hamutoko, J. T., Wanke, H., Gaj, M., and Koeniger, P.: Examination of deep root water
 545 uptake using anomalies of soil water stable isotopes, depth-controlled isotopic labeling and mixing
 546 models, *J. Hydrol.*, 566, 122–136, <https://doi.org/10.1016/j.jhydrol.2018.08.060>, 2018.
- 547 Beyer, M., Kühnhammer, K., and Dubbert, M.: In situ measurements of soil and plant water isotopes:
 548 a review of approaches, practical considerations and a vision for the future, *Hydrol. Earth Syst. Sci.*,
 549 24, 4413–4440, <https://doi.org/10.5194/hess-24-4413-2020>, 2020.
- 550 Burgess, S. S. O., Adams, M. A., Turner, N. C., and Ong, C. K.: The redistribution of soil water by
 551 tree root systems, *Oecologia*, 115, 306–311, <https://doi.org/10.1007/s004420050521>, 1998.
- 552 Caldwell, M. M. and Richards, J. H.: Hydraulic lift: water efflux from upper roots improves
 553 effectiveness of water uptake by deep roots, *Oecologia*, 79, 1–5, <https://doi.org/10.1007/BF00378231>,
 554 1989.
- 555 Campbell, G. S. and Norman, J.: *An Introduction to Environmental Biophysics*, Springer Science &
 556 Business Media, 296 pp., 2012.
- 557 Dawson, T. E. and Pate, J. S.: Seasonal water uptake and movement in root systems of Australian
 558 phraeatophytic plants of dimorphic root morphology: a stable isotope investigation, *Oecologia*, 107,
 559 13–20, <https://doi.org/10.1007/BF00582230>, 1996.



- 560 Fernandez-Tschieder, E., Marshall, J. D., and Binkley, D.: Carbon budget at the individual-tree scale:
 561 dominant Eucalyptus trees partition less carbon belowground, *New Phytol.*, 242, 1932–1943,
 562 <https://doi.org/10.1111/nph.19764>, 2024.
- 563 Gao, D., Joseph, J., Werner, R. A., Brunner, I., Zürcher, A., Hug, C., Wang, A., Zhao, C., Bai, E.,
 564 Meusburger, K., Gessler, A., and Hagedorn, F.: Drought alters the carbon footprint of trees in soils—
 565 tracking the spatio-temporal fate of ¹³C-labelled assimilates in the soil of an old-growth pine forest,
 566 *Glob. Change Biol.*, 27, 2491–2506, <https://doi.org/10.1111/gcb.15557>, 2021.
- 567 Drought reduces water uptake in beech from the drying topsoil, but no compensatory uptake occurs
 568 from deeper soil layers: <https://pub.epsilon.slu.se/26344/>, last access: 4 March 2022.
- 569 Gessler, A., Bächli, L., Rouholahnejad Freund, E., Treydte, K., Schaub, M., Haeni, M., Weiler, M.,
 570 Seeger, S., Marshall, J., Hug, C., Zweifel, R., Hagedorn, F., Rigling, A., Saurer, M., and Meusburger,
 571 K.: Drought reduces water uptake in beech from the drying topsoil, but no compensatory uptake
 572 occurs from deeper soil layers, *New Phytol.*, 233, 194–206, <https://doi.org/10.1111/nph.17767>, 2022.
- 573 Goldsmith, G. R., Allen, S. T., Braun, S., Engbersen, N., González-Quijano, C. R., Kirchner, J. W.,
 574 and Siegwolf, R. T. W.: Spatial variation in throughfall, soil, and plant water isotopes in a temperate
 575 forest, *Ecohydrology*, 12, e2059, <https://doi.org/10.1002/eco.2059>, 2019.
- 576 Gonfiantini, R.: Standards for stable isotope measurements in natural compounds, *Nature*, 271, 534–
 577 536, <https://doi.org/10.1038/271534a0>, 1978.
- 578 Göttlicher, S. G., Taylor, A. F. S., Grip, H., Betson, N. R., Valinger, E., Högberg, M. N., and
 579 Högberg, P.: The lateral spread of tree root systems in boreal forests: Estimates based on ¹⁵N uptake
 580 and distribution of sporocarps of ectomycorrhizal fungi, *For. Ecol. Manag.*, 255, 75–81,
 581 <https://doi.org/10.1016/j.foreco.2007.08.032>, 2008.
- 582 Guderle, M. and Hildebrandt, A.: Using measured soil water contents to estimate evapotranspiration
 583 and root water uptake profiles – a comparative study, *Hydrol. Earth Syst. Sci.*, 19, 409–425,
 584 <https://doi.org/10.5194/hess-19-409-2015>, 2015.
- 585 Guswa, A. J.: The influence of climate on root depth: A carbon cost-benefit analysis, *Water Resour.*
 586 *Res.*, 44, <https://doi.org/10.1029/2007WR006384>, 2008.
- 587 Gutierrez Lopez, J., Tor-ngern, P., Oren, R., Kozii, N., Laudon, H., and Hasselquist, N. J.: How tree
 588 species, tree size, and topographical location influenced tree transpiration in northern boreal forests
 589 during the historic 2018 drought, *Glob. Change Biol.*, 27, 3066–3078,
 590 <https://doi.org/10.1111/gcb.15601>, 2021.
- 591 Havranek, R. E., Snell, K. E., Davidheiser-Kroll, B., Bowen, G. J., and Vaughn, B.: The Soil Water
 592 Isotope Storage System (SWISS): An integrated soil water vapor sampling and multiport storage
 593 system for stable isotope geochemistry, *Rapid Commun. Mass Spectrom.*, 34, e8783,
 594 <https://doi.org/10.1002/rcm.8783>, 2020.
- 595 Henriksson, N., Lim, H., Marshall, J., Franklin, O., McMurtrie, R. E., Lutter, R., Magh, R.,
 596 Lundmark, T., and Näsholm, T.: Tree water uptake enhances nitrogen acquisition in a fertilized boreal
 597 forest – but not under nitrogen-poor conditions, *New Phytol.*, 232, 113–122,
 598 <https://doi.org/10.1111/nph.17578>, 2021.
- 599 Henriksson, N., Marshall, J., Högberg, M. N., Högberg, P., Polle, A., Franklin, O., and Näsholm, T.:
 600 Re-examining the evidence for the mother tree hypothesis – resource sharing among trees via
 601 ectomycorrhizal networks, *New Phytol.*, 239, 19–28, <https://doi.org/10.1111/nph.18935>, 2023.



- Herbstritt, B., Gralher, B., Seeger, S., Rinderer, M., and Weiler, M.: Technical note: Discrete in situ vapor sampling for subsequent lab-based water stable isotope analysis, *Hydrol. Earth Syst. Sci.*, 27, 3701–3718, <https://doi.org/10.5194/hess-27-3701-2023>, 2023.
- Jackson, R. B., Canadell, J., Ehleringer, J. R., Mooney, H. A., Sala, O. E., and Schulze, E. D.: A global analysis of root distributions for terrestrial biomes, *Oecologia*, 108, 389–411, <https://doi.org/10.1007/BF00333714>, 1996.
- Jocher, G., Marshall, J., Nilsson, M. B., Linder, S., De Simon, G., Hörnlund, T., Lundmark, T., Näsholm, T., Ottosson Löfvenius, M., Tarvainen, L., Wallin, G., and Peichl, M.: Impact of Canopy Decoupling and Subcanopy Advection on the Annual Carbon Balance of a Boreal Scots Pine Forest as Derived From Eddy Covariance, *J. Geophys. Res. Biogeosciences*, 123, 303–325, <https://doi.org/10.1002/2017JG003988>, 2017.
- Kakouridis, A., Hagen, J. A., Kan, M. P., Mambelli, S., Feldman, L. J., Herman, D. J., Weber, P. K., Pett-Ridge, J., and Firestone, M. K.: Routes to roots: direct evidence of water transport by arbuscular mycorrhizal fungi to host plants, *New Phytol.*, 236, 210–221, <https://doi.org/10.1111/nph.18281>, 2022.
- Klosterhalfen, A., Chi, J., Kljun, N., Lindroth, A., Laudon, H., Nilsson, M. B., and Peichl, M.: Two-level eddy covariance measurements reduce bias in land-atmosphere exchange estimates over a heterogeneous boreal forest landscape, *Agric. For. Meteorol.*, 339, 109523, <https://doi.org/10.1016/j.agrformet.2023.109523>, 2023.
- Kühnhammer, K., Dahlmann, A., Iraheta, A., Gerchow, M., Birkel, C., Marshall, J. D., and Beyer, M.: Continuous in situ measurements of water stable isotopes in soils, tree trunk and root xylem: Field approval, *Rapid Commun. Mass Spectrom.*, 36, e9232, <https://doi.org/10.1002/rcm.9232>, 2022.
- Kühnhammer, K., van Haren, J., Kübert, A., Bailey, K., Dubbert, M., Hu, J., Ladd, S. N., Meredith, L. K., Werner, C., and Beyer, M.: Deep roots mitigate drought impacts on tropical trees despite limited quantitative contribution to transpiration, *Sci. Total Environ.*, 893, 164763, <https://doi.org/10.1016/j.scitotenv.2023.164763>, 2023.
- Kuiper, L. C. and Coutts, M. P.: Spatial disposition and extension of the structural root system of Douglas-fir, *For. Ecol. Manag.*, 47, 111–125, [https://doi.org/10.1016/0378-1127\(92\)90269-F](https://doi.org/10.1016/0378-1127(92)90269-F), 1992.
- Kulmatiski, A., Beard, K. H., Verweij, R. J. T., and February, E. C.: A depth-controlled tracer technique measures vertical, horizontal and temporal patterns of water use by trees and grasses in a subtropical savanna, *New Phytol.*, 188, 199–209, <https://doi.org/10.1111/j.1469-8137.2010.03338.x>, 2010.
- Kulmatiski, A., Adler, P. B., and Foley, K. M.: Hydrologic niches explain species coexistence and abundance in a shrub–steppe system, *J. Ecol.*, 108, 998–1008, <https://doi.org/10.1111/1365-2745.13324>, 2020.
- Landgraf, J., Tetzlaff, D., Dubbert, M., Dubbert, D., Smith, A., and Soulsby, C.: Xylem water in riparian willow trees (*Salix alba*) reveals shallow sources of root water uptake by in situ monitoring of stable water isotopes, *Hydrol. Earth Syst. Sci.*, 26, 2073–2092, <https://doi.org/10.5194/hess-26-2073-2022>, 2022.
- Landwehr, J. M. and Coplen, T. B.: Line-conditioned excess: a new method for characterizing stable hydrogen and oxygen isotope ratios in hydrologic systems, *International Conference on Isotopes in Environmental Studies*, Monte-Carlo, Monaco, 132–135, 2006.



- 644 Lechthaler, S., Kiorapostolou, N., Pitacco, A., Anfodillo, T., and Petit, G.: The total path length's
645 hydraulic resistance according to known anatomical patterns: what is the shape of the root-to-leaf
646 tension gradient along the plant's longitudinal axis?, *J. Theor. Biol.*,
647 <https://doi.org/10.1016/j.jtbi.2020.110369>, 2020.
- 648 Lim, H., Oren, R., Palmroth, S., Tor-ngern, P., Mörling, T., Näsholm, T., Lundmark, T., Helmisaari,
649 H.-S., Leppälammil-Kujansuu, J., and Linder, S.: Inter-annual variability of precipitation constrains
650 the production response of boreal *Pinus sylvestris* to nitrogen fertilization, *For. Ecol. Manag.*, 348,
651 31–45, <https://doi.org/10.1016/j.foreco.2015.03.029>, 2015.
- 652 Lindroth, A., Holst, J., Linderson, M.-L., Aurela, M., Biermann, T., Heliasz, M., Chi, J., Ibrom, A.,
653 Kolari, P., Klemetsson, L., Krasnova, A., Laurila, T., Lehner, I., Lohila, A., Mammarella, I., Mölder,
654 M., Löfvenius, M. O., Peichl, M., Pilegaard, K., Soosaar, K., Vesala, T., Vestin, P., Weslien, P., and
655 Nilsson, M.: Effects of drought and meteorological forcing on carbon and water fluxes in Nordic
656 forests during the dry summer of 2018, *Philos. Trans. R. Soc. B Biol. Sci.*, 375, 20190516,
657 <https://doi.org/10.1098/rstb.2019.0516>, 2020.
- 658 Lutter, R., Henriksson, N., Lim, H., Blaško, R., Magh, R.-K., Näsholm, T., Nordin, A., Lundmark, T.,
659 and Marshall, J. D.: Belowground resource utilization in monocultures and mixtures of Scots pine and
660 Norway spruce, *For. Ecol. Manag.*, 500, 119647, <https://doi.org/10.1016/j.foreco.2021.119647>, 2021.
- 661 Lwila, A., Ammer, C., Gailing, O., Leinemann, L., and Mund, M.: Root overlap and allocation of
662 above- and belowground growth of European beech in pure and mixed stands of Douglas fir and
663 Norway spruce, *For. Ecosyst.*, 11, 100217, <https://doi.org/10.1016/j.fecs.2024.100217>, 2024.
- 664 Magh, R.-K., Gralher, B., Herbstritt, B., Kübert, A., Lim, H., Lundmark, T., and Marshall, J.:
665 Technical note: Conservative storage of water vapour – practical in situ sampling of stable isotopes in
666 tree stems, *Hydrol. Earth Syst. Sci.*, 26, 3573–3587, <https://doi.org/10.5194/hess-26-3573-2022>, 2022.
- 667 Mahall, B. E. and Callaway, R. M.: Root Communication Mechanisms and Intracommunity
668 Distributions of Two Mojave Desert Shrubs, *Ecology*, 73, 2145–2151,
669 <https://doi.org/10.2307/1941462>, 1992.
- 670 Majoube, M.: Fractionnement en oxygène 18 et en deutérium entre l'eau et sa vapeur, *J Chim Phys*,
671 68, 1423–1436, 1971.
- 672 Manoli, G., Bonetti, S., Domec, J.-C., Putti, M., Katul, G., and Marani, M.: Tree root systems
673 competing for soil moisture in a 3D soil–plant model, *Adv. Water Resour.*, 66, 32–42,
674 <https://doi.org/10.1016/j.advwatres.2014.01.006>, 2014.
- 675 Marshall, J. D.: Drought and shade interact to cause fine-root mortality in Douglas-fir seedlings, *Plant*
676 *Soil*, 91, 51–60, 1986.
- 677 Marshall, J. D., Brooks, J. R., and Lajtha, K.: Sources of variation in the stable isotopic composition
678 of plants, *Stable Isot. Ecol. Environ. Sci.*, 22–60, 2007.
- 679 Marshall, J. D., Cuntz, M., Beyer, M., Dubbert, M., and Kuehnhammer, K.: Borehole Equilibration:
680 Testing a New Method to Monitor the Isotopic Composition of Tree Xylem Water in situ, *Front. Plant*
681 *Sci.*, 11, <https://doi.org/10.3389/fpls.2020.00358>, 2020.
- 682 Marshall, J. D., Tarvainen, L., Zhao, P., Lim, H., Wallin, G., Näsholm, T., Lundmark, T., Linder, S.,
683 and Peichl, M.: Components explain, but do eddy fluxes constrain? Carbon budget of a nitrogen-
684 fertilized boreal Scots pine forest, *New Phytol.*, 239, 2166–2179, <https://doi.org/10.1111/nph.18939>,
685 2023.



- 686 Martin, F. M. and van der Heijden, M. G. A.: The mycorrhizal symbiosis: research frontiers in
687 genomics, ecology, and agricultural application, *New Phytol.*, 242, 1486–1506,
688 <https://doi.org/10.1111/nph.19541>, 2024.
- 689 McCulloh, K. A., Sperry, J. S., and Adler, F. R.: Water transport in plants obeys Murray’s law,
690 *Nature*, 421, 939–942, <https://doi.org/10.1038/nature01444>, 2003.
- 691 Mensah, C., Šigut, L., Fischer, M., Foltýnová, L., Jocher, G., Acosta, M., Kowalska, N., Kokrda, L.,
692 Pavelka, M., Marshall, J. D., Nyantakyi, E. K., and Marek, M. V.: Assessing the Contrasting Effects
693 of the Exceptional 2015 Drought on the Carbon Dynamics in Two Norway Spruce Forest Ecosystems,
694 *Atmosphere*, 12, 988, <https://doi.org/10.3390/atmos12080988>, 2021.
- 695 Moreira, M. Z., Sternberg, L. da S. L., and Nepstad, D. C.: Vertical patterns of soil water uptake by
696 plants in a primary forest and an abandoned pasture in the eastern Amazon: an isotopic approach,
697 *Plant Soil*, 222, 95–107, <https://doi.org/10.1023/A:1004773217189>, 2000.
- 698 Oerter, E. J. and Bowen, G.: In situ monitoring of H and O stable isotopes in soil water reveals
699 ecohydrologic dynamics in managed soil systems, *Ecohydrology*, 10, e1841,
700 <https://doi.org/10.1002/eco.1841>, 2017.
- 701 Plamboeck, A. H., Grip, H., and Nygren, U.: A hydrological tracer study of water uptake depth in a
702 Scots pine forest under two different water regimes, *Oecologia*, 119, 452–460,
703 <https://doi.org/10.1007/s004420050807>, 1999.
- 704 da S. L. Sternberg, L., Moreira, M. Z., and Nepstad, D. C.: Uptake of water by lateral roots of small
705 trees in an Amazonian Tropical Forest, *Plant Soil*, 238, 151–158, 2002.
- 706 Seeger, S. and Weiler, M.: Temporal dynamics of tree xylem water isotopes: in situ monitoring and
707 modeling, *Biogeosciences*, 18, 4603–4627, <https://doi.org/10.5194/bg-18-4603-2021>, 2021.
- 708 Shigo, A. L.: Compartmentalization: A Conceptual Framework for Understanding How Trees Grow
709 and Defend Themselves, *Annu. Rev. Phytopathol.*, 22, 189–214,
710 <https://doi.org/10.1146/annurev.py.22.090184.001201>, 1984.
- 711 Simard, S. W. and Durall, D. M.: Mycorrhizal networks: a review of their extent, function, and
712 importance, *Can. J. Bot.*, 82, 1140–1165, <https://doi.org/10.1139/b04-116>, 2004.
- 713 Sternberg, L. da S. L., Bucci, S., Franco, A., Goldstein, G., Hoffman, W. A., Meinzer, F. C., Moreira,
714 M. Z., and Scholz, F.: Long range lateral root activity by neo-tropical savanna trees, *Plant Soil*, 270,
715 169–178, <https://doi.org/10.1007/s11104-004-1334-9>, 2005.
- 716 Stocker, B. D., Tumber-Dávila, S. J., Konings, A. G., Anderson, M. C., Hain, C., and Jackson, R. B.:
717 Global patterns of water storage in the rooting zones of vegetation, *Nat. Geosci.*, 16, 250–256,
718 <https://doi.org/10.1038/s41561-023-01125-2>, 2023.
- 719 Tarvainen, L., Wallin, G., Lim, H., Linder, S., Oren, R., Ottosson Löfvenius, M., Rantfors, M., Tor-
720 ngern, P., and Marshall, J.: Photosynthetic refixation varies along the stem and reduces CO₂ efflux in
721 mature boreal *Pinus sylvestris* trees, *Tree Physiol.*, 38, 558–569,
722 <https://doi.org/10.1093/treephys/tpx130>, 2018.
- 723 Vernay, A., Tian, X., Chi, J., Linder, S., Mäkelä, A., Oren, R., Peichl, M., Stangl, Z. R., Tor-Ngern,
724 P., and Marshall, J. D.: Estimating canopy gross primary production by combining phloem stable
725 isotopes with canopy and mesophyll conductances, *Plant Cell Environ.*, 43, 2124–2142,
726 <https://doi.org/10.1111/pce.13835>, 2020.



- 727 Volkmann, T. H. M., Kühnhammer, K., Herbstritt, B., Gessler, A., and Weiler, M.: A method for in
 728 situ monitoring of the isotope composition of tree xylem water using laser spectroscopy, *Plant Cell*
 729 *Environ.*, 39, 2055–2063, <https://doi.org/10.1111/pce.12725>, 2016.
- 730 Werner, C., Meredith, L. K., Ladd, S. N., Ingrisich, J., Kübert, A., van Haren, J., Bahn, M., Bailey, K.,
 731 Bamberger, I., Beyer, M., Blomdahl, D., Byron, J., Daber, E., Deleeuw, J., Dippold, M. A., Fudyma,
 732 J., Gil-Loaiza, J., Honeker, L. K., Hu, J., Huang, J., Klüpfel, T., Krechmer, J., Kreuzwieser, J.,
 733 Kühnhammer, K., Lehmann, M. M., Meeran, K., Misztal, P. K., Ng, W.-R., Pfannerstill, E., Pugliese,
 734 G., Purser, G., Roscioli, J., Shi, L., Tfaily, M., and Williams, J.: Ecosystem fluxes during drought and
 735 recovery in an experimental forest, *Science*, 374, 1514–1518, <https://doi.org/10.1126/science.abj6789>,
 736 2021.
- 737 White, J. W. C., Cook, E. R., Lawrence, J. R., and Wallace S., B.: The DH ratios of sap in trees:
 738 Implications for water sources and tree ring DH ratios, *Geochim. Cosmochim. Acta*, 49, 237–246,
 739 [https://doi.org/10.1016/0016-7037\(85\)90207-8](https://doi.org/10.1016/0016-7037(85)90207-8), 1985.
- 740 Zhao, P., Chi, J., Nilsson, M. B., Löfvenius, M. O., Högberg, P., Jocher, G., Lim, H., Mäkelä, A.,
 741 Marshall, J., Ratcliffe, J., Tian, X., Näsholm, T., Lundmark, T., Linder, S., and Peichl, M.: Long-term
 742 nitrogen addition raises the annual carbon sink of a boreal forest to a new steady-state, *Agric. For.*
 743 *Meteorol.*, 324, 109112, <https://doi.org/10.1016/j.agrformet.2022.109112>, 2022.

744